ELSEVIER

Chemical Engineering Journal 119 (2006) 61–68

Chemical Engineering Journal

www.elsevier.com/locate/cej

Cr(VI) adsorption by waste acorn of *Quercus ithaburensis* in fixed beds: Prediction of breakthrough curves

Emine Malkoc [a,*], Yasar Nuhoglu [a], Yüksel Abali [b]

[a] *Department of Environmental Engineering, Faculty of Engineering, Atatürk University, 25240 Erzurum, Turkey*
[b] *Department of Chemistry, Faculty of Arts and Science, Celal Bayar University, 45030 Manisa, Turkey*

Received 31 May 2005; received in revised form 3 January 2006; accepted 23 January 2006

Abstract

The adsorption of Cr(VI) onto waste acorn of *Quercus ithaburensis* was studied using fixed-bed adsorption. The experiments were conducted to study the effect of important design parameters such as flow rate, solution pH and particle size of adsorbent. Decrease in adsorbent particle size and flow rate produced a better bed capacity. Also an increase in flow rate and particle size resulted in a decrease in the bed volumes at the breakthrough. The highest bed capacities of fixed-bed column were obtained at pH 2.0. In the beginning of all the pH experiments, the effluent pH increased dramatically and then dropped and approached lower values. The breakthrough data obtained for Cr(VI) was adequately described by the Thomas and Yoon–Nelson adsorption models. Good agreement between the predicted theoretical breakthrough curves and the experimental results were observed. This study indicated that the waste acorn of *Quercus ithaburensis* can be used as an effective and environmentally friendly adsorbent for the treatment of Cr(VI) containing wastewaters.

Keywords: *Quercus ithaburensis*; Chromium; Adsorption; Modeling; Fixed-bed column

1. Introduction

The removal of toxic heavy metals from aqueous streams is an important issue facing industries discharging effluents bearing heavy metals. The main sources of chromium pollution are mining, leather tanning, cement industries, electro plating, production of steel and other metal alloys, photographic material and corrosive paints [1]. *Hexavalent chromium*, Cr(VI), is a powerful carcinogenic agent that modifies the DNA transcription process causing important chromosomic aberrations. The Cr(VI) may also cause epigastric pain, nausea, vomiting, severe diarrhea, and hemorrhage [2].

Various treatment processes have been introduced for the removal of metal ions [3]. Current treatment processes include precipitation, oxidation/reduction, membrane filtration/osmosis, ion exchange and adsorption. Each process has its advantages and disadvantages, but ion exchange/adsorption methods do offer the most direct method of producing the highest quality treated water [4].

Activated carbon is a commonly used adsorbent for the removal of pollutants present in water and wastewater. In spite of its effectiveness in the removal of heavy metals from wastewaters, the high cost of activated carbon has restricted its more widespread use. Hence, an economical and easily available adsorbent would certainly make an adsorption-based process a viable alternative for the treatment of wastewater containing heavy metals [5]. The adsorption of Cr(VI) on persimmon tannin gel [6], sphagnum *moss peat* [7], fungus [8], sawdust [9] and distillery sludge [10] has been reported.

Batch reactors were easy to use in the laboratory study, but less convenient for industrial applications. On the other hand, fixed-bed columns were widely used in various chemical industries because of their operation [11]. The performance of packed beds is described through the concept of the breakthrough curve. The time for breakthrough appearance and the shape of the breakthrough curve are very important characteristics for determining the operation and the dynamic response of a adsorption column. The breakthrough curves show the loading behavior of metal to be removed from solution in a fixed bed and is usually expressed in terms of adsorbed metal concentration (C_{ad} = inlet metal concentration (C_0) − outlet metal concentration (C_t) or

* Corresponding author. Tel.: +90 442 2314606; fax: +90 442 2360957.
E-mail address: emalkoc@atauni.edu.tr (E. Malkoc).

1385-8947/$ – see front matter © 2006 Elsevier B.V. All rights reserved.
doi:10.1016/j.cej.2006.01.019

normalized concentration defined as the ratio of effluent metal concentration to inlet metal concentration (C_t/C_0) as a function of time or volume of effluent for a given bed height [12]. Effluent volume (V_{eff}) can be calculated from the following equation:

$$V_{eff} = Qt \quad (1)$$

where t and Q are the total flow time (min) and volumetric flow rate (ml min^{-1}). The area under the breakthrough curve (A) obtained by integrating the adsorbed concentration (C_{ad}; mg l^{-1}) versus t (min) plot can be used to find the total adsorbed metal quantity (maximum column capacity). Total adsorbed metal quantity (q_{total}; mg) in the column for a given feed concentration and flow rate is calculated from the following equation:

$$q_{total} = \frac{QA}{1000} = \frac{Q}{1000}\int_{t=0}^{t=t_{total}} C_{ad}\,dt \quad (2)$$

Equilibrium metal uptake (q_{eq}) (or maximum capacity of the column) in the column is defined by Eq. (3) as the total amount of metal sorbed (q_{total}) per gram of sorbent (X) at the end of total flow time [12].

$$q_{eq} = \frac{q_{total}}{X} \quad (3)$$

In the studies of fixed-bed adsorption processes, breakthrough and number of bed volumes are normally used in the description and comparison [13]. The breakthrough is usually defined as the phenomenon when the effluent concentration from the column is about 3–5% of the influent concentration [11,13]. The number of bed volumes (BV) is defined as:

$$\text{number of bed volumes} = \frac{\text{volume of solution treated}}{\text{volume of adsorbent bed}} = \frac{\text{operating time}}{\text{EBRT}} \quad (4)$$

The empty bed residence time EBRT is the time required for the liquid to fill the empty column [4]:

$$\text{EBRT} = \frac{\text{bed volume}}{\text{volumetric flow rate of the liquid}} \quad (5)$$

The adsorbent exhaustion rate is the mass of adsorbent used per volume of liquid treated at breakthrough [4]:

$$\text{adsorbent exhaustion rate} = \frac{\text{mass of adsorbent in column}}{\text{volume treated at breakthrough}} \quad (6)$$

2. Experimental

2.1. Adsorbent

The waste acorn of *Quercus ithaburensis* (an oak tree species) was produced by the tanning industry after tannin production from acorn which includes nut, cup and finger. It was produced and supplied from "Salihli Palamut ve Valeks Sanayi T.A.S." in Salihli, Manisa, Turkey. Decolorized and cleaned waste of acorn was dried at room temperature for a few days. It was ground in a blender and sieved to the desired particle size.

2.2. Column experiments

A schematic diagram for the pilot plant fixed-bed column systems is shown in Fig. 1. The fixed-bed columns were made of Perspex tubes 2.0 cm internal diameter and 30 cm in height. The bed length used in the experiments was 10 cm. In a typical experiment the metal of a known concentration was pumped at a fixed flow rate to the filled with known bed height of adsorbent. The particle size of adsorbent used in the experiment was 1.0–3.0 mm. The pH of the solutions was maintained constant at 2.0. The temperature of stream feeding solution and of the column was controlled at 25 °C through a thermostatic bath. The bed porosity was 0.23.

A stock Cr(VI) solution (1000 mg l^{-1}) was prepared in distilled water using $K_2Cr_2O_7$. All working solutions were prepared by diluting the stock solution with distilled water.

Liquid samples of the concentration of Cr(VI) in the exit of the column were collected at pre-defined time intervals. Cr(VI) concentration was then determined using an indirect UV–vis spectrophotometric method based on the reaction of Cr(VI) and diphenyl carbazid, which forms a red–violet colored complex. The absorbance of the colored complex was measured in a double beam spectrophotometer at 540 nm wavelength [14].

3. Results and discussion

3.1. SEM micrographic examinations

Scanning electron microscopy of adsorbent (waste acorn of *Quercus ithaburensis*) was carried out in a JEOL JSM T-330 unit. In order to see the surfaces of particles, SEM images were obtained for the raw and treated adsorbents. SEM images for the samples of the raw and treated materials are represented in Figs. 2 and 3, respectively.

A representative experiment under the given conditions such as 25 °C, pH 2.0, a contact time of 1440 min^{-1}, 0.5–1.0 mm of particle size, and an feed Cr(VI) concentration of 100 mg l^{-1} was carried out to obtain the micrograph in Fig. 3. It is clearly seen the surfaces of particles after adsorption in Fig. 3 that, the pores

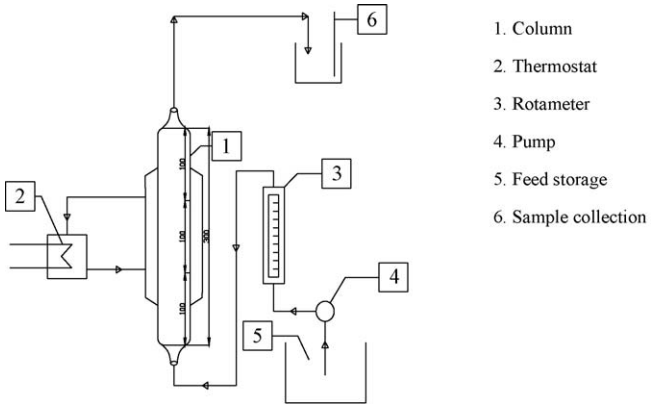

Fig. 1. Experimental system for fixed-bed operation. (1) Column; (2) thermostat; (3) rotameter; (4) pump; (5) feed storage; (6) sample collection.

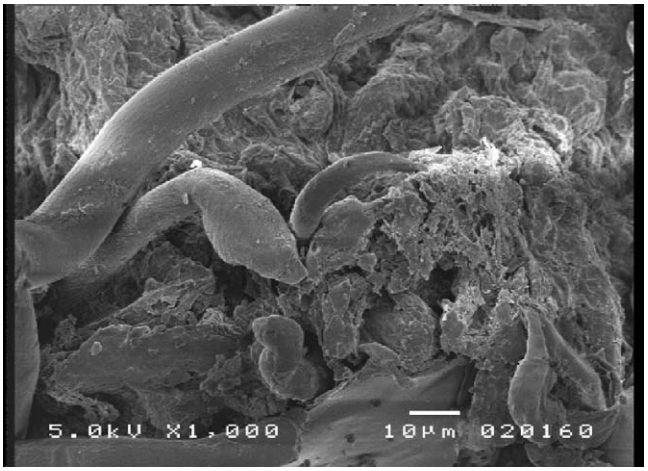

Fig. 2. SEM micrograph of the particles of waste acorn before Cr(VI) adsorption (particle size = 0.5–1.0 mm).

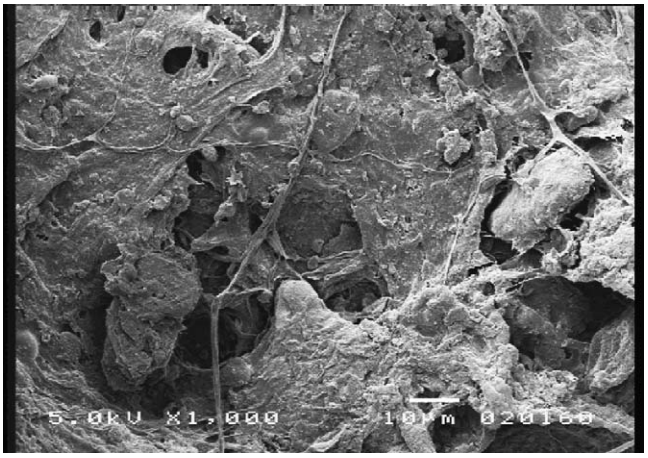

Fig. 3. SEM micrograph of the particles of waste acorn after Cr(VI) adsorption (pH 2.0, initial Cr(VI) concentration = 100 mg l^{-1}, particle size = 0.5–1.0 mm, flow rate = 10 ml min^{-1}).

and surfaces of adsorbent were covered and became smooth by adsorbate.

3.2. Fourier transform infrared spectroscopy (FTIR) analysis

The infrared spectra of the adsorbent sample was measured as potassium bromide pellets using a Perkin-Elmer 1600 series FTIR spectrometer. The FTIR spectra of the waste acorn are shown in Fig. 4.

As shown in the figure, the spectra display a number of absorption peaks, indicating the complex nature of waste acorn of *Quercus ithaburensis*. The bands at 3413 cm^{-1} representing bonded –OH groups. The bands observed at about 2924–2857 cm^{-1} could be assigned to the C–H stretch. The peaks around 1734 and 1625 correspond to the C=O stretch. The peaks observed at 1511 cm^{-1} correspond to the secondary amine group. Carboxylate ions gave rise to two bands: a strong symmetrical stretching band at 1451 and 1322 cm^{-1}, and a asymmetrical stretching band at 1380 cm^{-1}, respectively. The SO_3 stretching is observed at 1245 cm^{-1}. The C–O stretching of ether groups displays at the ranges of 1163 and 1105 cm^{-1}. The C–O band absorption peaks is observed to shift to 1050 and 1037 cm^{-1}. Thus, it seems that this type of functional group is likely to participate in metal binding. Among these absorption peaks especially the bonded –OH groups, C=0 stretching, secondary amine group and carboxyl groups were especially involved in chromium(VI) biosorption [15–19].

3.3. Effect of feed solution pH

The most important parameter influencing the sorption capacity is the pH of adsorption medium. The initial pH of adsorption medium is related to the adsorption mechanisms onto the adsorbent surface from water and reflects the nature of the physico-

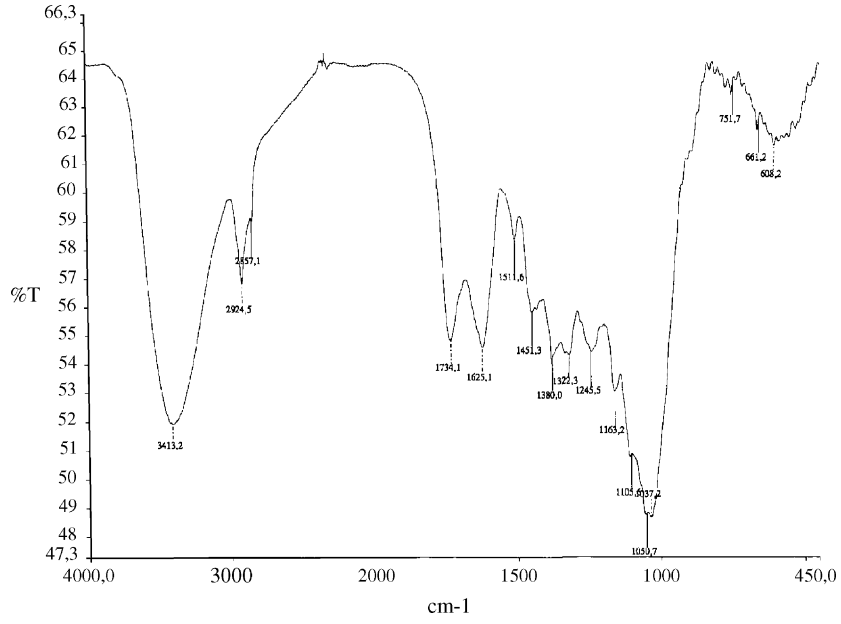

Fig. 4. FTIR spectrum of waste acorn.

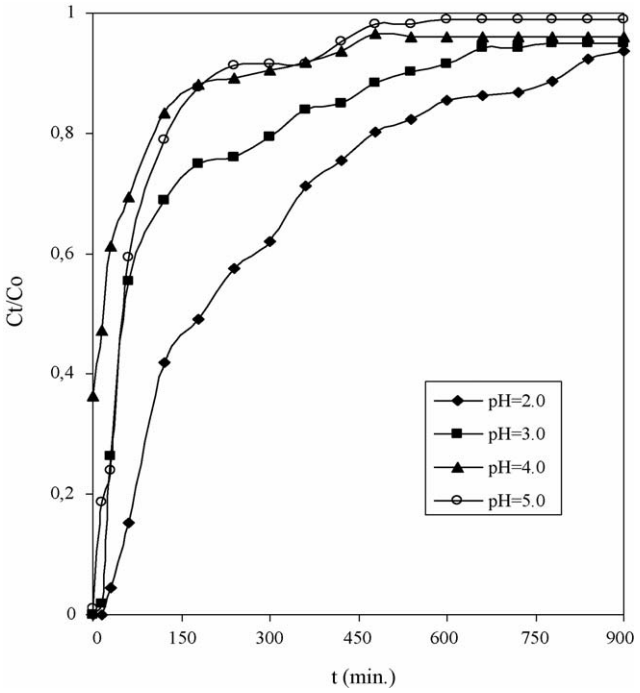

Fig. 5. Effect of feed solution pH on breakthrough curve (C_0 = 100 mg l^{-1}, flow rate = 10 ml min^{-1}, particle size = 1.0–3.0 mm, bed height = 10 cm, amount of adsorbent = 10 g).

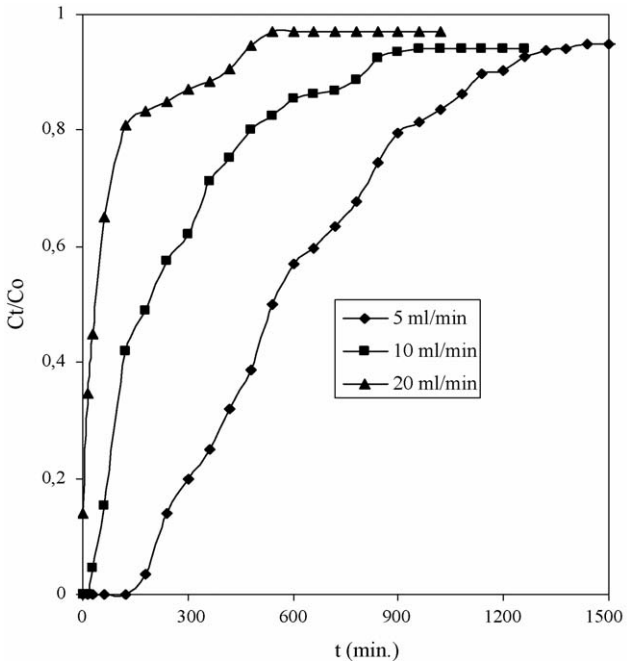

Fig. 6. Effect of flow rate on breakthrough curve (C_0 = 100 mg l^{-1}, pH of the solution = 2.0, particle size = 1.0–3.0 mm, bed height = 10 cm (10 g)).

chemical interaction of the species in solution and the adsorptive sites of adsorbent [12]. The pH of feed solution is an important controlling parameter in the heavy metal adsorption process and thus the role of hydrogen ion concentration was examined from solutions at different pH, covering a range of 2.0–5.0. In Cr(VI) adsorption on waste acorn, the highest maximum bed capacity and the longest breakthrough time is obtained at lowest pH value.

As seen from Fig. 5, an decrease in pH of feed solution increases the volume treated until breakthrough and the service time of the bed. Also, it was shown that with a decrease in the pH of feed solution, the breakthrough curves shifted from left to right, which indicated that more Cr(VI) ions were removed.

Cr(VI) exists in different forms in aqueous solution and the stability of these forms is dependent on the pH of the system. It is well known that the dominant form of Cr(VI) at pH 2.0–4.0 is the acid chromate ion species ($HCrO_4^-$) and increasing the pH will shift the concentration of $HCrO_4^-$ to other forms, CrO_2^{2-} and $Cr_2O_7^{2-}$ [20]. The highest bed capacity was obtained at pH 2.0. The amounts of Cr(VI) ions adsorbed per unit weight of beds for pH 2.0, 3.0, 4.0 and 5.0 were 26.65, 14.61, 6.31 and 7.72 mg g^{-1}, respectively. The breakthrough occurred 248 bed volume (BV) at pH 2.0 while that took place at 191.1 BV at pH 5.0. The empty bed contact time (EBCT) in pH experiment was 3.14 min. The more adsorbent usage rate was higher, the later time bed was saturated. At pH 2.0, adsorbent usage rate (1.28 g l^{-1}) and breakthrough time (960 min) was higher value.

A dramatic change in the effluent pH was observed in this study. For the influent solution with pH 2.0, 3.0, 4.0 and 5.0, the effluent pH was sharply increased to 5.1, 5.5, 6.3 and 6.0, respectively. It was that adsorption of hydrogen ions from the solution and dissolution of some impurities from the adsorbent surface could result in increase in the effluent pH [11]. As continued to flow through the column, the effluent pH dropped to the influent pH value.

3.4. Effect of flow rate

To investigate the effect of flow rate on the adsorption of Cr(VI) ions by waste *acorn* of *Quercus ithaburensis*, the inlet metal concentration in the feed was held constant at 100 mg l^{-1} while the flow rate was changed from 5 to 20 ml min^{-1}. Breakthrough curves, C_t/C_0 versus time is shown in Fig. 6 for three flow rates, 5, 10 and 20 ml min^{-1}.

As can be seen in Fig. 6, the bed capacities decreased with the increase in flow rate. The maximum bed capacities for flow rates, 5, 10 and 20 ml min^{-1} was found as 30.23, 26.65 and 15.98 mg g^{-1}, respectively. It was also found that the adsorbent gets saturated early at higher flow rate (20 ml min^{-1}). Also, as the flow rate increased, the breakthrough curve becomes steeper. The break point time and adsorbed ion concentration decreases. The reason for this behavior can be explained in the following way: if the residence time of the solute in the column is not long enough for adsorption equilibrium to be reached at that flow rate, the metal solution leaves the column before equilibrium occurs [21].

As shown in Fig. 6, the breakthrough occurs at 1440, 780 and 600 min for flow rate of 5, 10 and 20 ml min^{-1}, respectively. Accordingly, the breakthrough takes place at 458.6, 248, 191.1 BV for flow rate 5, 10 and 20 ml min^{-1}, respectively; the respective empty bed residence time(EBRT) are 6.28, 3.14 and 1.57 min. Also, as the flow rate increased, adsorbent exhaus-

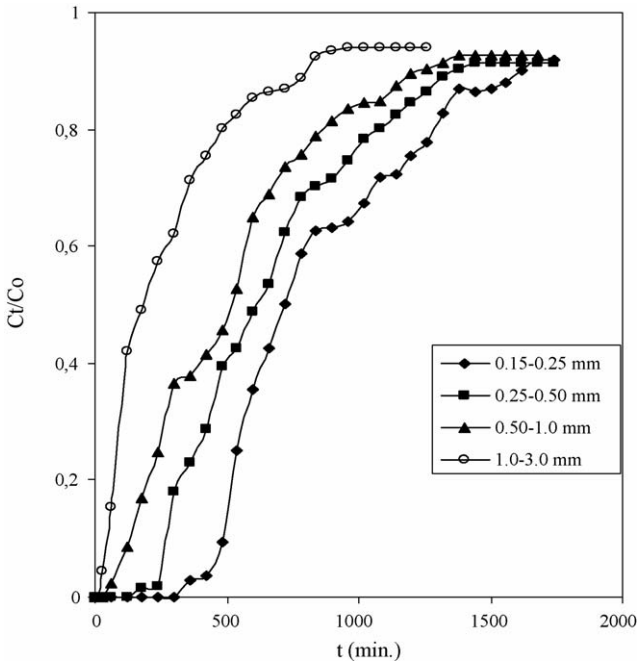

Fig. 7. Effect of particle size on breakthrough curve (C_0 = 100 mg l^{-1}, pH of the solution = 2.0, flow rate = 10 ml min^{-1}, bed height = 10 cm).

tion rate increased. Comparison of these values indicates that the treated bed volume (BV) increases with a higher EBRT. In other words, with a higher EBRT, Cr(VI) ions had more time to contact with waste acorn, which resulted in higher removal of Cr(VI) ions in fixed-bed columns.

3.5. Effect of particle size

The effect of varying particle size used during the fixed-bed experiments had an important effect on column performance. In the finer particle size ranges, adsorption breakthrough curves followed a much more efficient profile than larger particle size ranges, in that the breakthrough time increased and the curves tended towards the classic 'S' shape profile [22].

The influence of particle size on metal uptake was studied with particles in the size ranges 0.15–0.25 to 1.0–3.0 mm. Fig. 7 shows that increasing the size of adsorbent particles reduces the maximum bed capacities and breakthrough time. For tested different particle size, maximum bed capacities and breakthrough time at size range varies from 0.15–0.25 to 1.0–3.0 mm were 62.4, 52.13, 44.68, 26.65 mg g^{-1} and 1680, 1500, 1360, 780 min, respectively. Smaller particles will have a shorter diffusion path, thus allowing the adsorbate to penetrate deeper into the adsorbent particle more quickly. In addition, the total external surface area per unit volume for all smaller particle inside the column will be larger.

While 50% breakthrough of Cr(VI) at 0.15–0.25 mm particle size was 228.6 bed volumes, the bed saturated completely occurred at approximately 535 bed volumes. The bed volume decreased with the increase in adsorbent particle size. When the particle size was changed from 0.15–0.25 to 1.0–3.0 mm, used bed volume decreased from 535 to 248 BV. Also, as the particle size of adsorbent increased, adsorbent exhaustion rate increased. While adsorbent exhaustion rate was 0.85 g l^{-1} at 0.15–0.25 mm particle size, adsorbent exhaustion rate obtained at 1.0–3.0 mm particle size of used adsorbent was increased 1.28 g l^{-1}. At all experiments, EBRT value is 3.14 min.

4. Modeling of the breakthrough curves

Adsorption operation is a complex process and its performance is governed by many variables. The outlet concentration from fixed bed is one of the important performance parameters of practical importance to the process designer. Prediction of the outlet concentration is not easy [23]. The maximum bed capacity of an adsorption column is needed in design. The Thomas model is used to fulfil the purpose. The Thomas solution is one of the most general and widely used methods in column performance theory. The model has the following form:

$$\frac{C_t}{C_0} = \frac{1}{1 + \exp\left(\frac{k_{TH}}{Q}(q_0 X - C_0 V_{eff})\right)} \quad (7)$$

where k_{TH} is the Thomas rate constant (ml min^{-1} mg^{-1}); q_0 the maximum solid-phase concentration of the solute (mg g^{-1}), V_{eff} the effluent volume (ml); X the mass of adsorbent (g); Q the flow rate (ml min^{-1}).

The kinetic coefficient k_{TH} and the adsorption capacity of the bed q_0 can be determined from a plot of $\ln[(C_0/C_t) - 1]$ against t at a given flow rate.

Yoon and Nelson model is based on the assumption that the rate of decrease in the probability of adsorption for each adsorbate molecule is proportional to the probability of adsorbate adsorption and the probability of adsorbate breakthrough on the adsorbent. The Yoon and Nelson equation regarding to a single-component system is expressed as;

$$\ln\frac{C_t}{C_0 - C_t} = k_{YN}t - \tau k_{YN} \quad (8)$$

where k_{YN} is the rate constant (l min^{-1}); τ the time required for 50% adsorbate breakthrough (min); t the breakthrough time (min).

The kinetic coefficient k_{YN} and τ can be determined from a plot of $\ln[C_t/(C_0 - C_t) - 1]$ against t at a given adsorption conditions. If the theoretical model accurately characterizes the experimental data, this plot will result in a straight line with slope of k_{YN} and intercept τk_{YN} [12].

The breakthrough curves showed the superposition of experimental results (points) and the theoretical calculated points(lines). Linear regression coefficients (R^2) showed the fit between experimental data and linearized forms of Thomas and Yoon–Nelson equations while the average percentage errors (ε%) calculated according to Eq. (9) indicated the fit between the experimental and predicted values of C_t/C_0 used for plotting

Table 1
Parameters predicted from the Thomas model and model deviations for Cr(VI) adsorption to waste acorn of *Quercus ithaburensis* at different flow rates and particle sizes

Q (ml min^{-1})	Particle size (mm)	k_{TH} (ml min^{-1} mg^{-1})	$q_{0,cal}$ (mg g^{-1})	$q_{0,exp}$ (mg g^{-1})	R^2	ε%
5	1.0–3.0	0.00004	33.50	30.23	0.948	4.30
10	1.0–3.0	0.00005	27.23	26.65	0.847	9.26
20	1.0–3.0	0.00008	12.28	15.98	0.838	9.91
10	0.15–0.25	0.00004	62.76	62.74	0.854	30.85
10	0.25–0.50	0.00004	61.31	52.13	0.846	26.22
10	0.50–1.0	0.00004	45.65	44.68	0.901	20.04

breakthrough curves.

$$\varepsilon = \frac{\sum_{i=1}^{N}\left[\frac{(C_t/C_0)_{exp}-(C_t/C_0)_{theo}}{(C_t/C_0)_{exp}}\right]}{N} \times 100 \quad (9)$$

where N is the number of measurements.

4.1. Application of the Thomas model

The column data were fitted to the Thomas model to determine the Thomas rate constant (k_{TH}) and maximum solid-phase concentration of the solute (q_0) and shown in Table 1.

As flow rate increased, the values of k_{TH} increased and the values of q_0 decreased. The bed capacity q_0 decreased and the coefficient k_{TH} not changed with increasing particle size of waste *Quercus ithaburensis*. It is clear from Fig. 8 that there is good agreement between the experimental and the predicted values at all flow rate. The data in Table 1 also show a negligible difference between the experimental and predicted values of bed capacity, the experimental values were less than 1% lower than the predicted values for Cr(VI) at all the flow rates. This result suggest that the Thomas model is valid for chromium(VI) adsorption in a waste acorn of *Quercus ithaburensis*.

The experimental and predicted breakthrough curves at different particle sizes are given in Fig. 9. In addition, although the deviations of experimental and predicted values were quite high, there was a good agreement between the experimental and predicted bed capacities at all particle size. The correlation coefficients were between 0.846 and 0.901 at tested particle size.

4.2. Application of the Yoon–Nelson model

A simple theoretical model developed by Yoon–Nelson was applied to investigate the breakthrough behavior of Cr(VI) on waste acorn of *Quercus ithaburensis*. The values of k_{YN} and τ were determined at different flow rates varied between 5 and 20 ml min^{-1} and at different particle sizes varied between 0.15–0.25 and 1.0–3.0 mm. These values were used to calculate the breakthrough curve.

From linearized Thomas equation plots, the correlation coefficients (R^2), average percentage errors (ε%), k_{YN} and τ_{cal} were

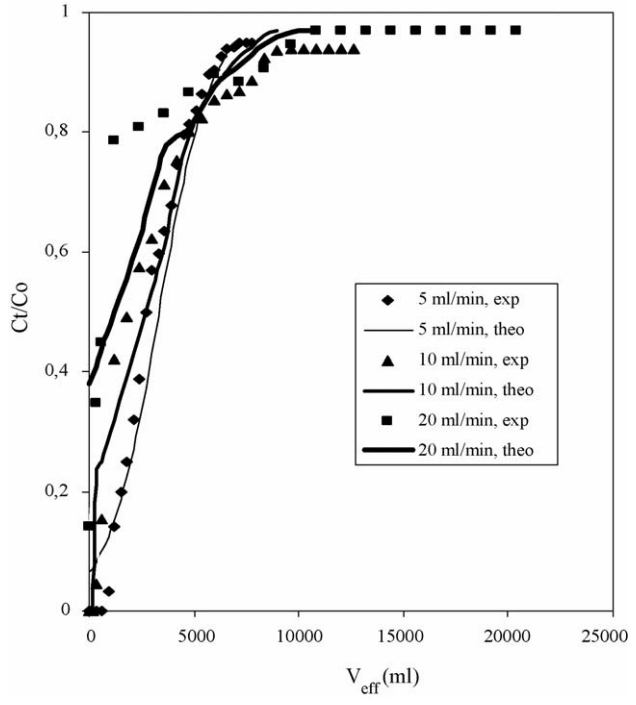

Fig. 8. Comparison of the experimental and predicted breakthrough curves obtained at different flow rates according to the Thomas model (C_0 = 100 mg l^{-1}, pH of the solution = 2.0, particle size = 1.0–3.0 mm, bed height = 10 cm).

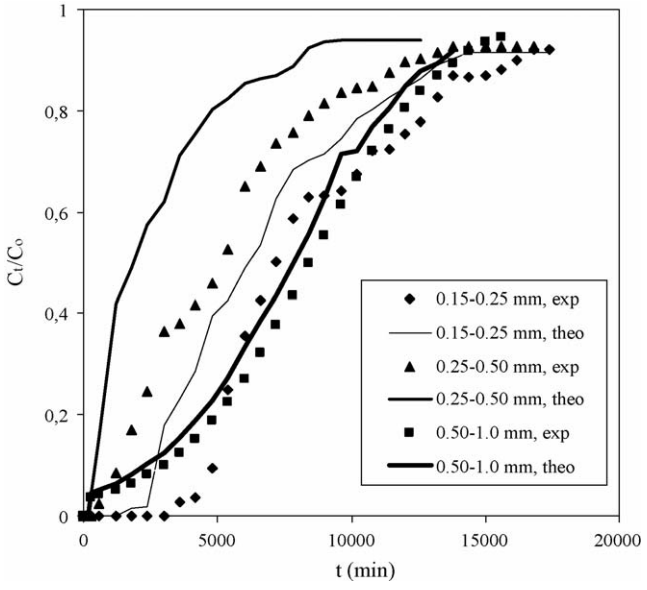

Fig. 9. Comparison of the experimental and predicted breakthrough curves obtained at different particle sizes according to the Thomas model (C_0 = 100 mg l^{-1}, pH of the solution = 2.0, flow rate = 10 ml min^{-1}, bed height = 10 cm).

Table 2
Parameters predicted from the Yoon–Nelson model and model deviations for Cr(VI) adsorption to waste *Quercus ithaburensis* at different flow rates and particle sizes

Q (ml min^{-1})	Particle size (mm)	k_{YN} (l min^{-1})	τ_{cal} (min)	τ_{exp} (min)	R^2	ε%
5	1.0–3.0	0.0035	545	542	0.992	8.40
10	1.0–3.0	0.0041	214	189	0.920	35.60
20	1.0–3.0	0.0071	35	39	0.779	5.55
10	0.15–0.25	0.0024	707	718	0.984	16
10	0.25–0.50	0.0032	652	617	0.974	17.58
10	0.50–1.0	0.0033	502	529	0.960	7.80

calculated for tested experimental parameters and are shown in Table 2. As shown in Table 2, k_{YN} increased and τ decreased with both increasing flow rate and particle size of adsorbent.

The correlation coefficients between the experimental and predicted values using Yoon–Nelson model for all tested flow rates were between 0.7790–0.9918 and 0.9200–0.9840 for all tested particle sizes. The data in Table 2 also indicated that calculated τ values are similar to experimental τ values.

The calculated breakthrough curve and experimental breakthrough curves at different flow rate and particle size are given Figs. 10 and 11. As shown Figs. 10 and 11, the experimental breakthrough curves were very close to calculated ones according to Yoon–Nelson model. From the experimental results and predicted values, the model proposed by Yoon–Nelson provided a very good correlation at tested flow rate and particle size.

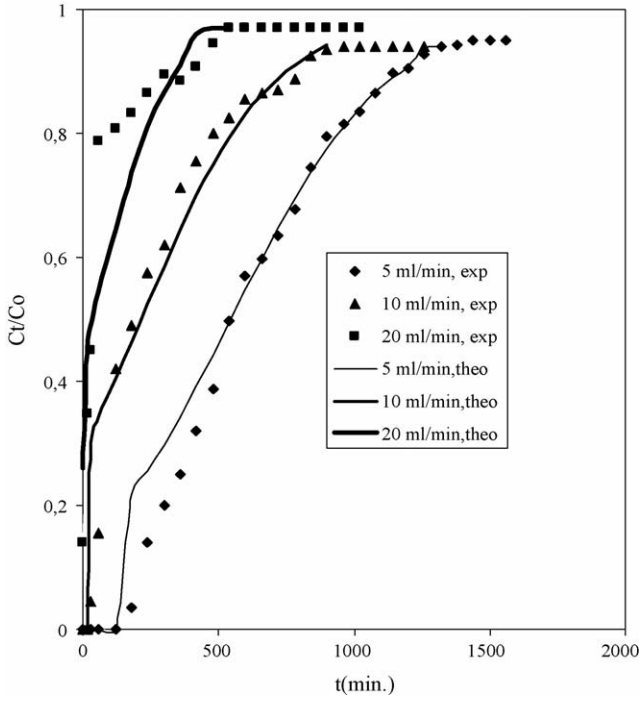

Fig. 10. Comparison of the experimental and predicted breakthrough curves obtained at different flow rates according to the Yoon–Nelson model (C_0 = 100 mg l^{-1}, pH of the solution = 2.0, particle size = 1.0–3.0 mm, bed height = 10 cm).

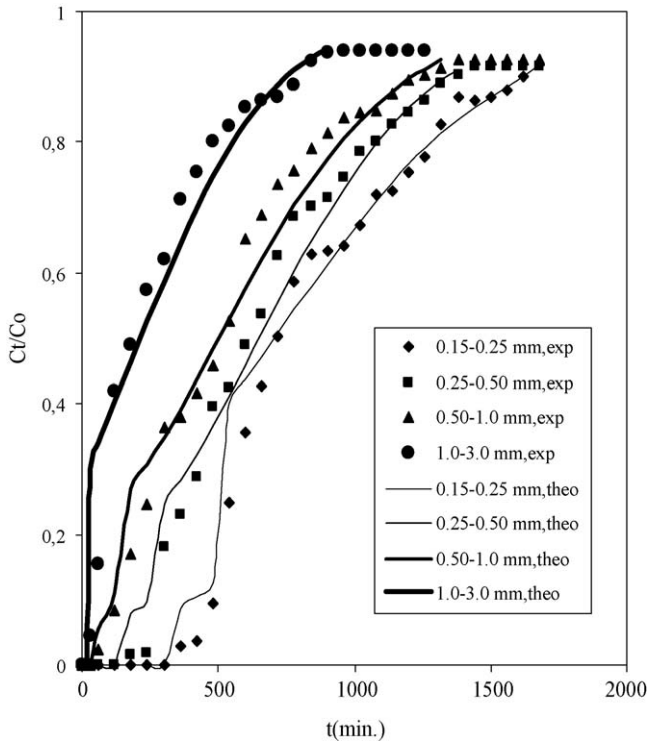

Fig. 11. Comparison of the experimental and predicted breakthrough curves obtained at different particle sizes according to the Yoon–Nelson model (C_0 = 100 mg l^{-1}, pH of the solution = 2.0, flow rate = 10 ml min^{-1}, bed height = 10 cm).

5. Conclusion

The present investigation aimed the heavy metal sorption from synthetic wastewaters with another pollutant matter. For this reason, the Cr(VI) removal from aqueous solutions through waste acorn of *Quercus ithaburensis* may be evaluated as an environmentally friendly and extra economic treatment. These studies show that waste acorn is an effective and inexpensive adsorbent for chromium(VI) removal from aqueous solutions. In fixed-bed column, the adsorption capacity is strongly dependent on the flow rate, pH of solution and particle size. The bed volumes slightly increased as flow rate and particle size was decreased. As the flow rate increased, the breakthrough curve became steeper, the break point time and adsorbed ion concentration decreased. With an increase in influent pH, the bed volumes treated decreased. In addition, the bed volumes slightly increased as flow rate and particle size were decreased. Thomas and Yoon–Nelson model were used in analysis of column performance data and the model parameters were evaluated. The calculated theoretical breakthrough curves were in good agreement with the corresponding experimental data.

Acknowledgement

This research was supported by the Research Project Unit at the Atatürk University under the project no. 2002/147.

References

[1] E. Malkoc, Y. Nuhoğlu, The removal of chromium(VI) from synthetic wastewater by *Ulothrix zonata*, Fresen. Environ. Bull. 12 (4) (2003) 376–381.

[2] M. Dakiky, M. Khamis, A. Manassra, M. Mer'eb, Selective adsorption of Cr(VI) in industrial wastewater using low-cost abundantly available adsorbents, Adv. Environ. Res. 6 (2002) 533–540.

[3] Z. Zulfadhly, M.D. Mashitah, S. Bhatia, Heavy metals removal in fixed-bed column by the macro fungus *Pycnoporus sanguineus*, Environ. Pollut. 112 (2001) 463–470.

[4] D.C.K. Ko, J.F. Porter, G. McKay, Optimized correlations for the fixed-bed adsorption of metal ions on bone char, Chem. Eng. Sci. 55 (2000) 5819–5829.

[5] T. Mathialagan, T. Viraraghavan, Adsorption of cadmium from aqueous solutions by perlite, J. Hazard. Mater. B94 (2002) 291–303.

[6] A. Nakajima, Y. Baba, Mechanism of hexavalent chromium adsorption by persimmon tannin gel, Water Res. 38 (2004) 2859–2864.

[7] D.C. Sharma, C.F. Forster, Removal of hexavalent chromium using sphagnum moss peat, Water Res. 27 (1993) 1201–1208.

[8] N. Tewari, P. Vasudevan, B.K. Guha, Study on biosorption of Cr(VI) by *Mucor hiemalis*, Biochem. Eng. J. 23 (2005) 185–192.

[9] N.K. Hamadi, X.D. Chen, M.M. Farid, M.G.Q. Lu, Adsorption kinetics for the removal of chromium(VI) from aqueous solution by adsorbents derived from used tyres and sawdust, Chem. Eng. J. 84 (2001) 95–105.

[10] K. Selvaraj, V. Chandramohan, S. Pattabhi, Removal of hexavalent chromium using distillery sludge, Bioresource Technol. 89 (2) (2003) 207–211.

[11] J.P. Chen, X. Wang, Removing copper, zinc and lead ion by granular activated carbon in pretreated fixed bed columns, Sep. Purif. Technol. 19 (2000) 157–167.

[12] Z. Aksu, F. Gönen, Biosorption of phenol by immobilized activated sludge in a continuous packed bed: prediction of breakthrough curves, Process Biochem. 39 (2004) 599–613.

[13] J.P. Chen, J.T. Yoon, S. Yiacoumi, Effects of chemical and physical properties of influent on copper sorption onto activated carbon fixed-bed columns, Carbon 41 (2003) 1635–1644.

[14] F.N. Acar, E. Malkoc, The removal of chromium (VI) from aqueous solutions by *Fagus orientalis* L., Bioresource Technol. 94 (1) (2004) 13–15.

[15] P.X. Sheng, Y.-P. Ting, J.P. Chen, L. Hong, Sorption of lead, copper, cadmium, zinc, and nickel by marine algal biomass: characterization of biosorptive capacity and investigation of mechanisms, J. Colloid Interf. Sci. 275 (2005) 131–141.

[16] I. Villaescusa, N. Fiol, M. Martínez, N. Miralles, J. Poch, J. Serarols, Removal of copper and nickel ions from aqueous solutions by grape stalks wastes, Water Res. 38 (2005) 992–1002.

[17] S.S. Ahluwalia, D. Goyal, Removal of heavy metals by waste tea leaves from aqueous solution, Eng. Life Sci. 5 (2005) 158–162.

[18] D. Park, Y.-S. Yun, J.M. Park, Studies on hexavalent chromium biosorption by chemically-treated biomass of *Ecklonia* sp, Cemosphere 60 (2005) 1356–1364.

[19] E. Malkoc, Y. Nuhoglu, Removal of Ni(II) ions from aqueous solutions using waste of tea factory: adsorption on a fixed-bed column, J. Hazard. Mater. doi:10.1016/j.jhazmat.2005.11.070.

[20] Z. Aksu, U. Acikel, E. Kabasakal, S. Tezer, Equilibrium modeling of individual and simultaneous biosorption of chromium (VI) and nickel (II) onto dried activated sludge, Water Res. 36 (12) (2002) 3063–3073.

[21] S. Ghorai, K.K. Pant, Investigations on the column performance of fluoride adsorption by activated alumina in a fixed-bed, Chem. Eng. J. 98 (1/2) (2004) 165–173.

[22] G.M. Walker, L.R. Weatherley, Adsorption of acid dyes on to granular activated carbon in fixed beds, Water Res. 31 (8) (1997) 2093–2101.

[23] S.H. Lin, R.S. Juang, Y.H. Wang, Adsorption of acid dye from water onto pristine and acid-activated clays in fixed beds, J. Hazard. Mater. B 113 (2004) 195–200.